An investigation of passive scalar transport in canopy turbulence using LDA and LIF

by

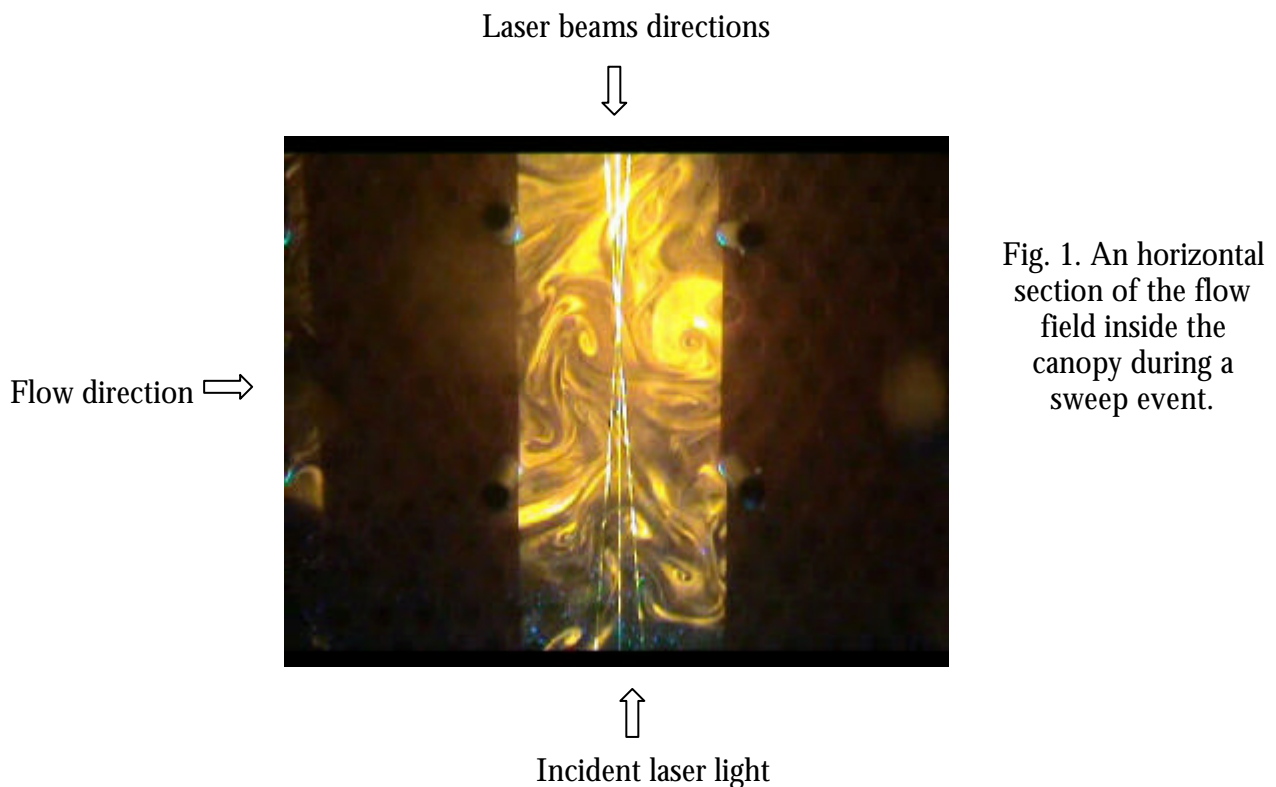D. Poggi[1,2,3] , M. Deval[1], L. Ridolfi[1], A. Porporato[2], J. Albertson[2,3] and G. Katul[2,3]

1) Dipartimento di Idraulica, Trasporti ed Infrastrutture Civili, Politecnico di Torino, Torino, Italy

2) Dep. of Civil and Environmental Engineering, Pratt School of Engineering, Duke University, Durham, U.S.A.

3) Nicholas School of the Environment and Earth Sciences, Duke University, Durham, U.S.A.

E-mail: davide.poggi@duke.edu, davide.poggi@polito.it

ABSTRACT

The problem of transport and diffusion of passive scalars in canopy sublayer (e.g. forests, urban canopies, vegetated channels) is of great interest in several fields. Although the main features of the flow field above and inside a dense canopy is now well understood (Finnigan, 2000; Raupach et al., 1996), the role of the principal vorticity (e.g. Kelvin-Helmholtz vorticity at the top of the canopy, *KH*, and von Karman vorticity inside the canopy, *vK*) in the transport and diffusion of passive scalar in canopy turbulence is still an open problem. In the present paper, Laser Induced Fluorescence (*LIF*) and Laser Doppler Anemometry (*LDA*) techniques are used simultaneously to study statistically the features of *KH* vorticity and their connection with the transport of passive scalar from above to inside a dense model canopy.

Detailed measurements are presented for the mean velocity (U), turbulent intensity of longitudinal and vertical velocity fluctuation (u, v), Reynolds stress ($\overline{uv}$), and mean and fluctuation concentration intensity (C, c). We show that, through the accurate choice of fluorescent dye and source laser, it is possible to obtain sufficiently high quality joint statistics ($\overline{uc}$ and $\overline{vc}$) without adopting complicate techniques of acquisition. Using this technique a new and more detailed analysis, at least in a statistical sense, of the flow field inside the canopy sublayer is possible. In particular, we show that inside the canopy the PDF of the vertical and longitudinal velocity associated with the shedding vorticity is well described by a Gaussian distribution. Otherwise, the sweep events, associated with the instability of Kelvin-Helmholtz vorticity, exhibit a PDF of the velocity that is well described by a gamma distribution.

Laser beams directions

Flow direction

Fig. 1. An horizontal section of the flow field inside the canopy during a sweep event.

Incident laser light

1. INTRODUCTION

The study of scalar transport and dispersion above and inside the canopy sublayer (*CSL*) is a crucial research problem in fluid dynamics, surface hydrology, and ecology (Baldocchi, 1992; Nathan, 2002; Wilson and Zhuang, 1989, Scanlon and Albertson, 2001). Although the main features of the flow field above and inside a dense canopy is now well understood (Finnigan, 2000; Raupach et al., 1996), the role of the principal vortices (e.g. Kelvin-Helmholtz vorticity) in the transport of passive scalar from outside to inside the canopy is still not clear. This lack of knowledge is due to the complex and non-linear interaction between several types of vortices that characterize the vorticity in the *CSL* (Poggi et al. 2004a). In particular, the region above the canopy is dominated by large eddies of size comparable with the canopy height. These eddies are due to the strong velocity gradient at the top of the canopy and show some dynamical features of KH vorticity (Raupach et al., 96). Otherwise, in the region inside the canopy the turbulence field is dominated (in time) by small vorticity of size comparable with the canopy elements scale (Raupach 1982, Poggi, 2004b). This vorticity, called von Karman vorticity, is due to the work done by the mean flow against form drag and it injects short-circuited turbulent kinetic energy into the flow field behind the canopy elements at the scales of the wakes. Intermittently the flow field inside the canopy is swept up by the large-scale vorticity induced by the instability of the KH at the canopy top (Raupach et al., 1996; Katul et al., 1998). This phenomenon, called sweep-ejection cycle, is of crucial importance because it is responsible for most of the mass, energy and scalars transfer from above to inside the canopy.

It is evident that, to deal with scalar transport and diffusion in canopy turbulence, a deeper analysis of the dynamics of the turbulent flow field is strongly needed. In fact, the transport processes are closely connected with the vorticity types both through the different dynamics of the vortices and through different regions of the canopy sub-layer (*CSL*) (in terms of scalar sources and sinks). For example, although the concentration distributions from a source releases close to the ground (e.g. forest floor respiration) is mainly subjected to the longitudinal von Karman vorticity, its behavior is intermittently and abruptly altered by strong ejection or sweep events due to the *KH* vorticity. Otherwise, the concentration distributions from a source releases near the canopy top (e.g. O_3 deposition) is mainly influenced by the transport and diffusion process due to the *KH* vortices but suddenly modify by their instability.

The first approach to study the complex interactions between these several types of coherent structures is to develop a detailed parameterization of turbulent transport processes within the canopy volume and near the canopy-atmosphere interface. To this goal, a complete understanding of the statistical property of the flow field, analyzing with particular care the features of the coherent structures, is essential. For example, turbulent dispersion analysis, such as Lagrangian stochastic models (LSM), can usefully employ a deep, if not complete, knowledge of the flow field statistics. As noted by Wilson and Sawford (1995) to have a basic knowledge of the flow statistics is more and more need to evaluate the single-point pdf of the Eulerian velocity field as a matematically-prescribed function of position. The knowledge of the exact, or at least well approximated, pdf could likely improve the prediction of the LS models. Nevertheless, the experimental analysis inside a canopy sublayer, needed to study the sweep-ejection cycle, is a very difficult problem to deal with because of the particular features of the flow field. In fact the *CSL* is inhomogeneous, non-local, non-Gaussian, highly dissipative and intermittent, thereby possing unique challenges to the classical experimental techniques available in canopy turbulence, such as LDA and hotwire in laboratory or sonic anemometer in the field experiments.

It is now well understood that using only a single point measurements, even in a very simple boundary condition such as a smooth wall, and despite the fact that many techniques have been developed (Antonia, 1981; Alfredsson and Johansson, 1984; Tardu, 1995; Porporato, 1999), the identification of the vortices or coherent structures is a far from simple operation. The reason lies in a interconnected set of problems: 1) coherent and non-coherent components in a turbulent field co-exist and dynamically interact (Hussain 1986), 2) most of the conditional techniques require an arbitrary calibration (Antonia, 1981) 3) the single point analysis of the turbulent flow field is often subject to spurious detection (Bogard and Tiederman, 1986). Moreover, in *CSL*, because of the wide range of time and length scales of the involved vortices and their complex interaction, a global spatial vision of the canopy turbulence dynamic is fundamental to understand the vorticity of the flow field. Nevertheless, the classical PIV or LIF, that have been expressly created to sample a wide region of the flow field, are not capable to resolve the high Reynolds number typical of canopy turbulence. Otherwise, the LDA can deal with very high Reynolds numbers but it resolves the flow field only in a single point. We choose to use simultaneously the LIF and the LDA in order to make

the most of both these techniques. In particular, the LIF guarantees a good identification of the events and the LDA a high sampling frequency of longitudinal and vertical velocity.
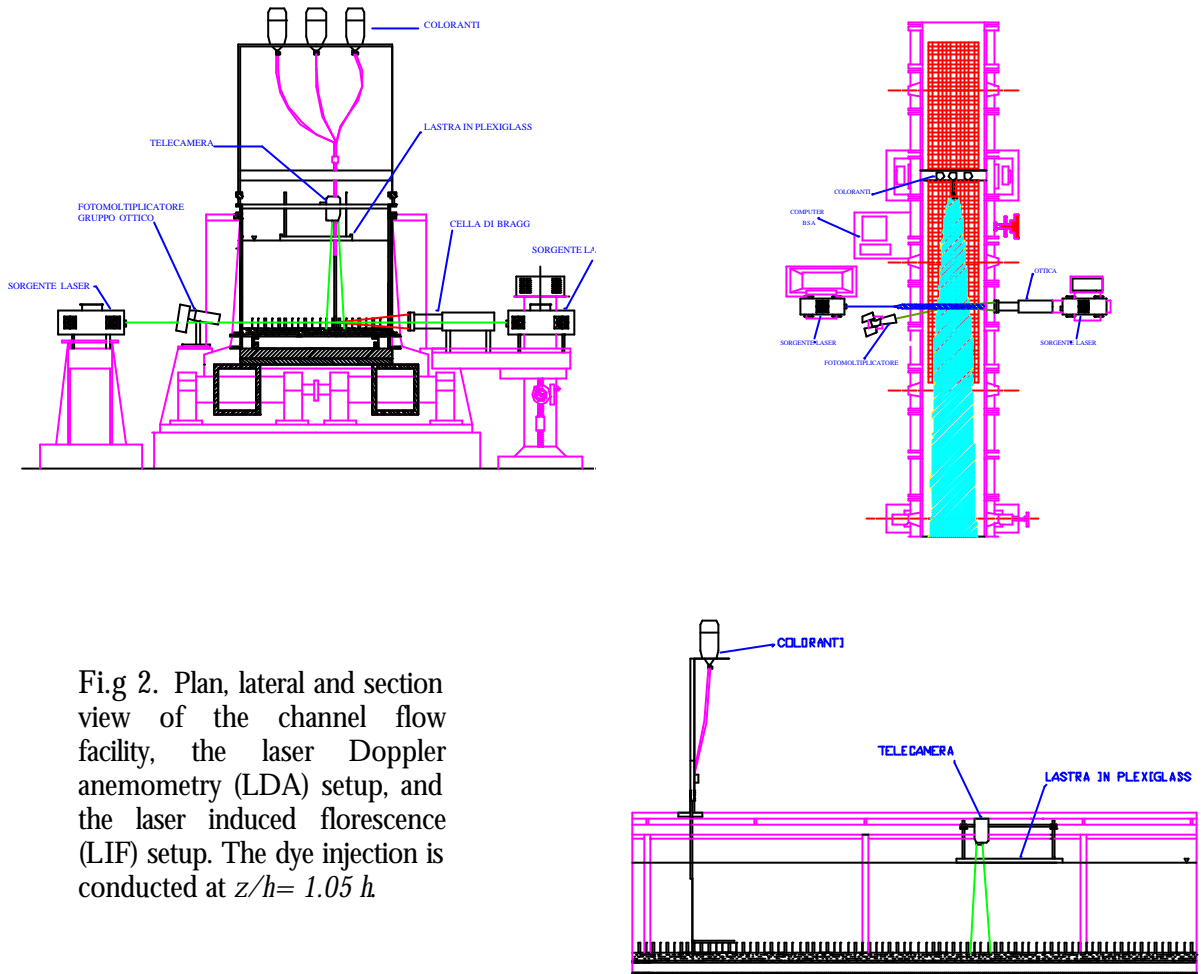

Fi.g 2. Plan, lateral and section view of the channel flow facility, the laser Doppler anemometry (LDA) setup, and the laser induced florescence (LIF) setup. The dye injection is conducted at *z/h= 1.05 h*.

2. EXPERIMENTAL FACILITIES AND SET-UP

The experiment was conducted at the hydraulics Laboratory, DITIC Politecnico di Torino, in a recirculating constant head flume shown schematically in Fig.2. The main part of the facility consists of a large rectangular channel 18 m long, 0.90 m wide, and 1 m deep. The walls are made of glass to allow the passage of laser light. The canopy is placed in a test section 9 m long and 0.9 m wide situated 7 m downstream from the channel entrance. The canopy is composed of an array of vertical steel cylinders, 12 cm tall (h), and 4 mm in diameter (d_r) arranged in a regular pattern with a density of 1072 rods m^{-2}. According to Poggi et al. (2004), such a density is dynamically equivalent to a dense canopy having an element area index (frontal area per unit volume) of 4.27 m^{2}m^{-3}. The test section begins 7 m downstream from the channel entrance. The rods were firmly installed into two parallel steel sheets drilled with evenly spaced holes. A polyurethane board was placed between the two sheets to further increase the rigidity of the rods. The measurements of these flow statistics, described next, were conducted after the flow attained a uniform state at a water depth of 60 cm.

The velocity was measured by two-component Laser Doppler Anemometry (*LDA*) used in forward scattering mode. A key advantage of *LDA* is its non-intrusive nature, its small averaging volume, and its ability to measure velocity excursions close to obstacles. The signal processing was performed by two Dantec Burst Spectrum Analyzer (*BSA*) processors. The coincidence mode was used to obtain more reliable measurements of the Reynolds shear stress. To preserve the correlation coefficient between the vertical (w) and the longitudinal (u) velocity components, all data points not exactly temporally coincident were discarded. Further details about the LDA configuration and signal processing can be found in Poggi et al. (2002). To compare the flow statistics across different canopy densities, the flow Reynolds number was preserved by varying the volumetric flow rate but retaining the water depth (=h_w) at a steady 60 cm.

2.1 Velocity Measurements.

The velocity was measured by two-component LDA used in forward scattering mode. A key advantage of LDA is its non-intrusive nature, its small averaging volume, and its ability to measure velocity close to the cylinders. The signal processing was performed by two Dantec Burst Spectrum Analyzer (BSA) processors. The coincidence mode was used to obtain more reliable measurements of the Reynolds shear stress. To preserve the correlation coefficient between the longitudinal and vertical velocity component, u and w respectively, all data points not exactly temporally coincident were discarded. Further details about the LDA configuration and signal processing can be found in Poggi et al. (2002). The sampling duration and frequency per run were 3600 s and 2500-3000 Hz, respectively. The analog signals from the processor were checked by an oscilloscope to verify the Doppler signal quality at each runs. No artificial seeding of the channel was employed. The bulk Reynolds number, Re_b, calculated using the vertically-averaged velocity (U_b) across h, is *116,000* which ensures fully-developed turbulence.

2.2 Scalar Concentration Measurements.

The planar LIF technique is employed to measure the local instantaneous dye concentration in the flow. This technique is based on the capacity of certain dye to react with fluorescence when excited by a laser sheet. The light is absorbed by the dye and it is emitted at a longer wavelength. The powerfulness of this technique is that the intensity of the emitted light is linearly proportional to the local dye concentration.

The light source is a 300 mW continuous fixed wavelength ion-argon laser (Melles Griot mod. 543-A-A03). A lens system, providing a 0.6 mm thick light sheet of about 60 cm in height and 25 cm in width, was used. To capture the rule of the sweep events in the transport of scalars from above to inside the canopy, the concentration were measured by injecting a dye solution, Fluorescein and Rhodamine 6G, through slits at the canopy top (z/h=1.05). The laser sheet, parallel to the bottom and transverse to the mean flow, was placed between to lines of rods at *z/h=0.3*. An example of the laser sheet and fluorescent dye during a sweep event is shown in figure 1; the orange area denotes the fluid carried by the coherent structure from the top of the canopy. The emitted light is directly proportional to the local concentration of the dye. The instantaneous planar distribution of the emitted light is recorded with a commercial digital color CCD video camera. This video set-up allowed us to store directly the digital movies with high resolution (720 x 480 pixels, DV-AVI with NTSC format) and high frequency (30 frames per second) without postprocessing the movie. A 12 min long video sequence was collected and was used to compute the scalar concentration statistics for the two source releases.

The usual approach to analyze the visualisation is converting each frame in a matrix having 256 grey levels. Once the relation between the grey levels (proportional to the dye fluorescent intensity) and the dye concentration is established, the concentration can be determined (H. Rehab et al. 2000). This technique is accurate if the measured light is only emitted by the fluorescent dye. In many practical applications the reflection effects of boundary conditions, such as the rods and the channel bottom in our experimental set-up, may introduce a high level of noise. To overcome this difficulty a more meticulous digital analysis of the frames is necessary. Nevertheless, in our case the digital color management is relatively simple because applied to imaging system that is restricted to only few types of inputs and outputs. The goal of the digital color analysis is to extract from each frame, through an ad-hoc calibration of the colors, only the light emitted by the fluorescent dye. Theoretically, because this light has a predominant wavelength (see fig. 3), the distinction between the fluorescent light and the noise should be very easy. Nevertheless, digital cameras may not encode the light at every wavelength. A densitometric color encoding, based on input-image color measurements made according to defined sets of spectral responsivities, is often used. The digital camera that we used encodes the colors in terms of red, green, and blue (RGB) densities.

The calibration of the colors is done plotting in a three dimensional RGB space the colors of each frame and analyzing the spacial distribution of the points. The points belonging to the dye emission will be distributed around a direction that is characteristic of the predominant wavelength of the fluorescent dye (fig. 4). In particular the projection of the points on the RB plane (fig. 4a) is particularly useful to distinguish between light noise and fluorescent light. Thanks to this peculiarity an easy postprocessing of the digital movie was carried out. In particular, the fluorescent intensity is proportional to the length of the vector having the selected direction in the RGB space.

Once the digital postprocessing is done, a relationship between the intensity level of the emitted light and the mean concentration is necessary. Four solutions with different known concentrations of dye were prepared in a small square tank. For each dye concentration, a short video was recorded and analyzed. In our case, the dye concentration was far from the saturation limit and the well-known linearity of the remitted light with dye concentration was applicable. This linearity also implies that four concentration levels were sufficient to calibrate the relation between concentration and light intensity.

2.2 **Simultaneous Measurements.**

The LDA and LIF techniques were used simultaneously to measure the local instantaneous concentration, c(t) and velocity, *u(t)* and *v(t)*, in the same point. Several problems of compatibility between LIF and LDA may arise when these two methods are used together.

The main problem was the alteration of the velocity signal induced by the dye energy emissions. To overcome this problem several fluorescent dyes were taken into consideration and the final choice was the carboxyrhodamine 6G (*CR 6G*). The choice of this fluorescent dye is motivated both by the excellent match to the 514 nm spectral line of the laser sheet and the falling between those of fluorescein and tetramethylrhodamine (530-650 nm). This peculiar range avoid the interaction of emitted fluorescent light with the LDA photomultipliers, that work at 514 nm and 488 nm respectively (see Fig. 3). In fact the energy that is emitted by the *CR 6G* can be filtered by the filters mounted on the photomultipliers. To check the capability of this method to acquire reliable velocity time series, several velocity measurements were carried out with and without laser sheet and with and without dye. In all these cases the times series showed the same velocity statistics.
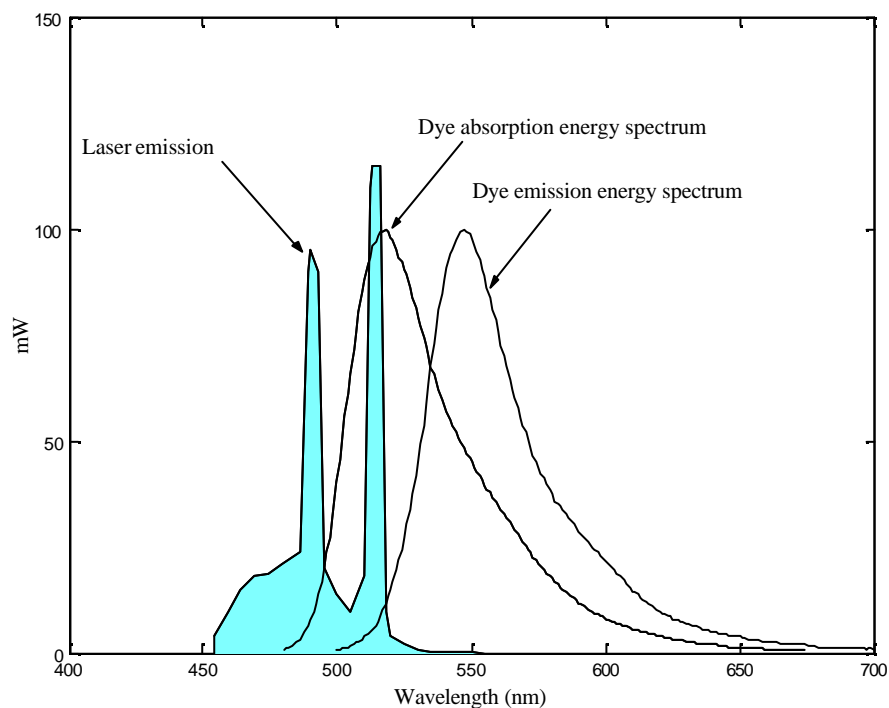
Fig. 3. The spectra of the dye absorption and emission togheter with the spectrum of the laser emission. Note the good matching between the second peak in the laser emission (514 nm) and the peak in the dye absorption.

A second problem arises because of the horizontal laser beams interference in the movie. In fact, the horizontal laser beams, having the same wavelength as the laser sheet and a saturating energy, induced a couple of thin lines in each movie frame (see Fig. 1). Therefore, instead to evaluate $\overline{uc}$ in the same point, the concentration was evaluated in two points: the first just before and the second just after the measurement location. The average between the first and the second point was used to estimate $\overline{uc}$. Through the analysis of a movie acquired without the LDA we made sure that this procedure was capable to produce a good estimate of the time signal in the measurement point. Similarly, the reliability of the proposed techniques was checked by comparing the first four moments of the velocity time series acquired with and without the dye injection.
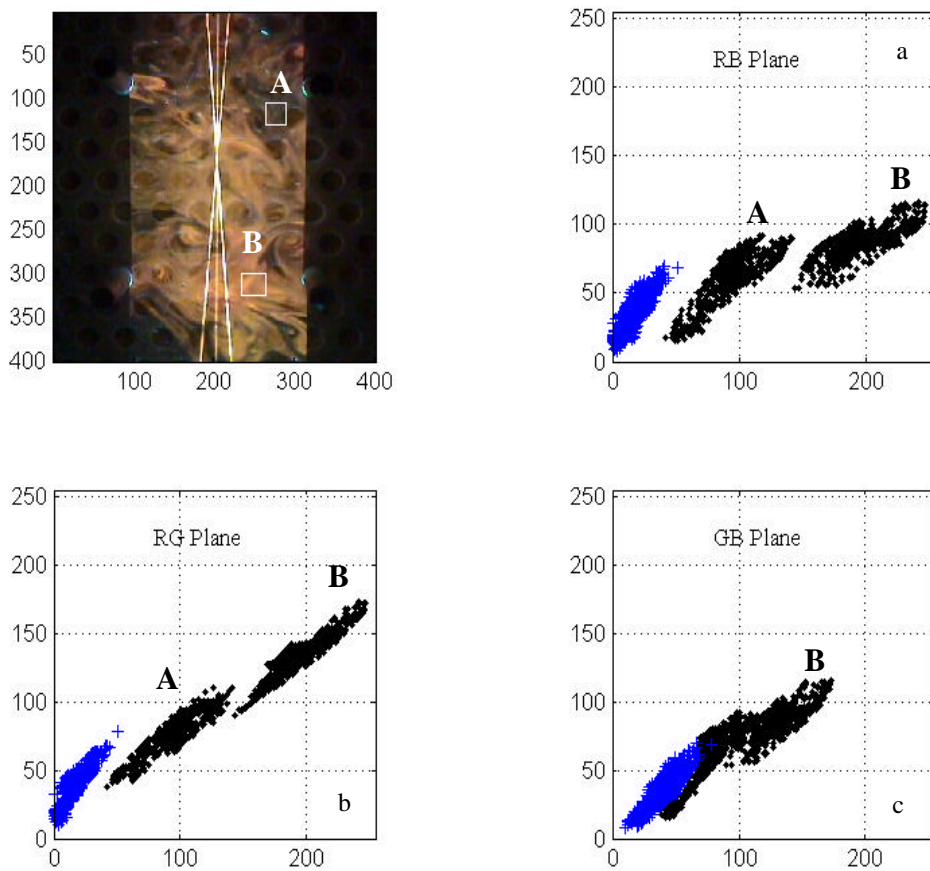

Fig. 4. An example of the 3D RGB matrix during a sweep event. The color components of the two points A and B (25 by 25 pixel^2) are especially discernible in the RB plane (a). For comparison, we show the points associated to the flow field without dye (blu crosses).

3. RESULTS

The analysis was carried out injecting a fluorescent dye at the top of the canopy and analyzing the contribution of the sweep events, the principal means of transport of passive scalar in canopy turbulence, to $\overline{uv}$, $\overline{uc}$, and $\overline{vc}$ inside

6

the canopy. In this way, because only the flow field above the canopy was marked, it was possible to analyze the Kelvin-Helmholtz instability, from which the sweeps are generated, separately from the von Karman vorticity that is directly created inside the canopy (Poggi et al. 2004). Firstly we tested the proposed method comparing the first four statistics of the vertical and longitudinal velocity with some field and laboratory experiments in literature (Finnigan, 2000; Poggi et al. 2004). Although the comparison of the statistics of $uc(t)$ is not possible because of the lack of results in literature, the presence of the classical ramps in the measured signal is an encouraging outcome. The good agreement between our results and the field and laboratory experiments gives some general confidence in the adopted canopy set up and in the suggested technique. Subsequently, the contribution of the sweep events to transport of momentum and passive scalars were studied. Through the analysis of the time series $uc(t)$ and $vc(t)$ it was possible to extract from the original time series of $u(t)$ and $v(t)$ the values belonged to the sweep events, $u_s(t)$ and $v_s(t)$. This analysis was carried out using the classical quadrant analysis applied to the plan u-c. Figure 4 shows the plan u-c and the thresholds that we used. Even without the chose of a threshold the points belonging to the sweep events are well discernable. In fact, while the most part of the points are distributed around the horizontal axis ($c=0$), the sweep events are characterized by strong longitudinal velocity and high concentration level (I quadrant). It is evident that the extraction of the velocity from the original time series is pretty easy and does not depend on the choice of the threshold level. An example extracted from the original time series $uc(t)$ is shown in figure 5 together with the selected time series of $u_s(t)$ and $c(t)$.
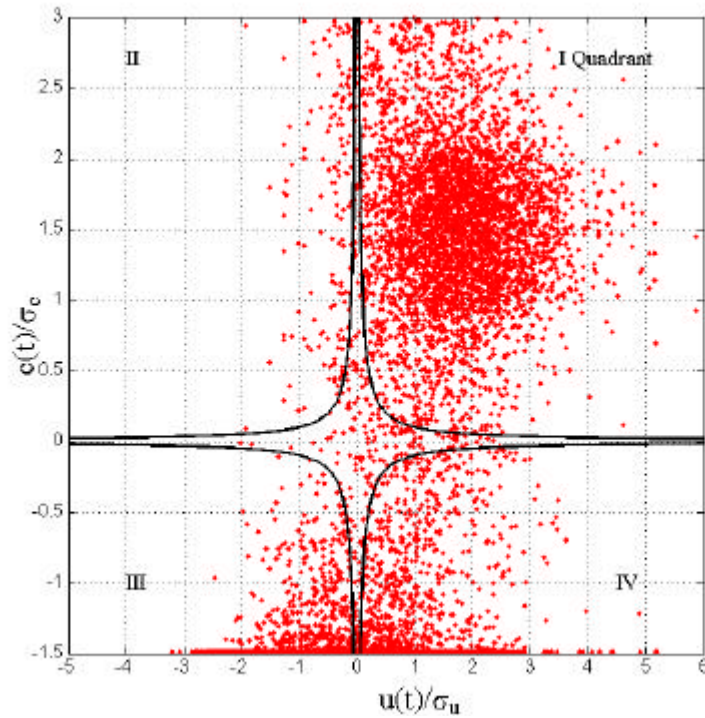

Fig. 5. The distribution of $u(t)$-$c(t)$ in the u-c plane. The points belong to the sweep events are well discernible on the I quadrant. Most of the other events are distribuited around the horizontal ($c=0$) axis.

Through the analysis of the time series we computed the joint probability distributions (JPDF) of longitudinal and vertical velocity amongst the contribution of sweep events and von Karman vorticity. In figure 5 the PDF of $u_s(t)$ is shown together with the PDF of the original time series, $u(t)$ and the PDF of a one hour long series of the longitudinal velocity acquired without both the laser sheet and the dye injection. Although, as expected, the PDF's definition of

$u(t)$ is not as high as the PDF of the longer time series, the good agreement support the robustness of the suggested technique.

As figure 5 shows while the PDF of sweeps events, $u(t)_s$, is well described through a gamma distribution (the solid line in figure 5), the remaining part of the original time series, $u(t)$, is better described through a gaussian distribution. This result is of great interest in the closure of both eulerian and lagrangian models (Reynolds, 1997). For example, turbulent dispersion analysis, such as Lagrangian stochastic models (LSM), can usefully employ a deep, if not complete, knowledge of the flow field statistics. As noted by Wilson and Sawford (1995) to have a basic knowledge of the flow statistics is more and more need to evaluate the single-point pdf of the Eulerian velocity field as a matematically-prescribed function of position. The knowledge of the exact, or well approximated, pdf could likely improve the prediction of the LS models.
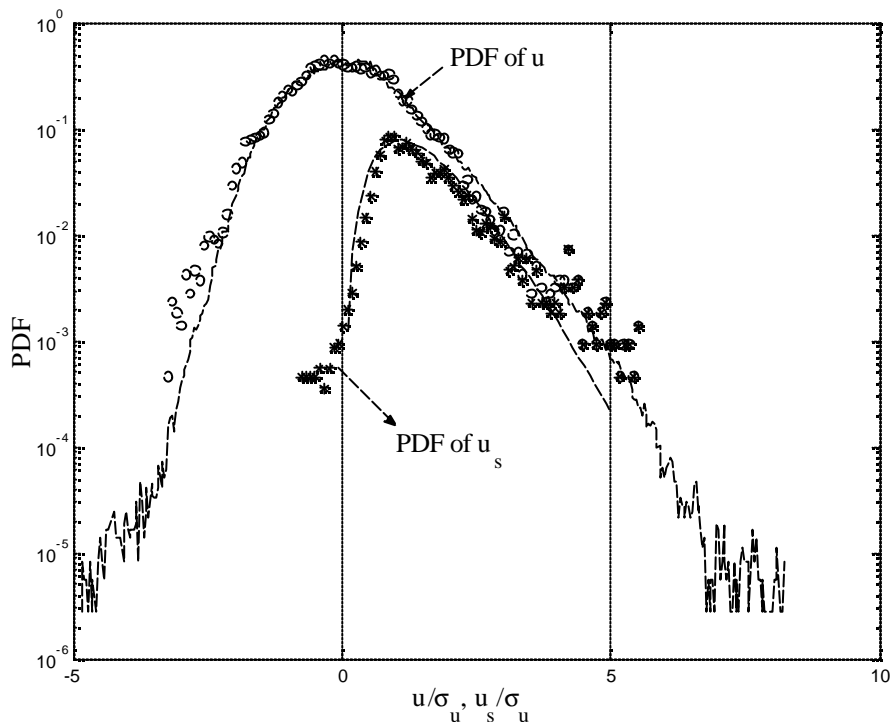

Fig. 6. The PDFs of the original, $u(t)$ (open cyrcles), and selected time series $u_s(t)$ (full cyrcles). For comparison, the PDF of one-hour long time series acquired without dye injection is also shown (dotted line).

4. CONCLUSIONS

Laser Induced Fluorescence (*LIF*) and Laser Doppler Anemometry (*LDA*) techniques were used simultaneously to study statistically the features of *KH* vorticity and their connection with the transport of passive scalar from inside a dense model canopy. Through the accurate choice of fluorescent dye and source laser and an ad hoc postprocessing of the *LIF* results, it is possible to obtain an high quality joint statistics ($\overline{uc}$ and $\overline{vc}$) without adopting complicate techniques of acquisition. Using this technique a new and deeper vision, at least in a statistical sense, of the flow field inside the canopy sublayer is possible. We show that inside the canopy the PDF of the vertical and longitudinal

8

velocity associated with the sweep events is well described by a gamma distribution. Otherwise, the shedding vorticity inside the canopy exhibits a PDF of the velocity that is well described by a Gaussian distribution.

REFERENCES

Alfredsson P.H. and Johansson A.V. (1984). "On the detection of turbulence-generating events", J Fluid Mech 139, pp 325-345.

Antonia R.A. (1981). "Conditional sampling in turbulence measurement", Ann. Rev. Fluid. Mech. 13, pp 131-156

Baldocchi, D. (1992). "A lagrangian random-walk model for simulating water-vapor, Co_2 and sensible heat-flux densities and scalar profiles over and within a soybean canopy", Boundary-Layer Meteorol. 61, pp 113-144.

Bogard D.G. and Tiederman W.G. (1986). "Burst detection with single-point velocity measurements", Journal of Fluid Mech. 162, pp 389-413.

Finnigan, J. (2000). "Turbulence in plant canopies", Ann. Rev. Fluid. Mech. 32, pp 519-571.

Katul, G., Geron, C., Hsieh, C., Vidakovic, B., and Guenther, A. (1998). "Active turbulence and scalar transport near the forest-atmosphere interface", J. Appl. Meteorol. 37, pp 1533-1546.

Nathan, R., Katul, G., Horn, H., Thomas, S., Oren, R., Avissar, R., Pacala, S., and Levin, S. (2002). "Mechanisms of long-distance dispersal of seeds by wind", Nature 418, pp 409-413.

Poggi, D., Porporato, A., and Ridolfi, L. (2002). "An experimental contribution to near-wall measurements by means of a special laser Doppler anemometry technique", Exp. Fluids 32, pp 366-375.

Poggi, D., Porporato, A., Ridolfi, L., Katul, and G., Albertson, J., (2004a). "Interaction between large and small scales in the canopy sublayer", Geoph. Research letters Vol. 31, L05102.

Poggi, D., Porporato, A., Ridolfi, L., Katul, and G., Albertson, J., (2004b). "The effect of vegetation density on canopy sublayer turbulence", Boundary-Layer Meteorol., 111 pp 565-587.

Porporato, A., (1999). "Conditional sampling and state space reconstruction", Exp. In Fluids, 26 pp 441-450.

Raupach, M., Finnigan, J., and Brunet, Y., (1996). "Coherent eddies and turbulence in vegetation canopies: The mixing-layer analogy", Boundary-Layer Meteorol. 78, pp 351-382.

H. Rehab, R. A. Antonia, A, L. Djenidi, L., Mi, J., (2000), "Characteristics of fluorescein dye and temperature fluctuations in a turbulent near-wake", Experiments in Fluids 28, pp 462-470.

Scanlon, T. and Albertson, J., (2001). "Turbulent transport of carbon dioxide and water vapor within a vegetation canopy during unstable conditions: Identification of episodes using wavelet analysis", J. Geophys. Res. 106, pp 7251-7262.

Tardu S., (1995). "Characteristics of single and clusters of bursting events in the inner layer; Part 1: Vita events", Exp Fluids 20, pp 112-124

Wilson, J., Zhuang, Y. (1989). "Restriction on the timestep to be used in stochastic lagrangian models of turbulent dispersion", Boundary-Layer Meteor. 49, pp 309-316.

Wilson, J. and Sawford, B. (1996). "Review of Lagrangian stochastic models for trajectories in the turbulent atmosphere", Boundary-Layer Meteorol. 78, pp 191-210.